



**HAL**  
open science

## A miniature biomimetic gaze control system

S. Viollet, N. Franceschini

► **To cite this version:**

S. Viollet, N. Franceschini. A miniature biomimetic gaze control system. IEEE International Conference on Robotics and Automation, 2004. Proceedings. ICRA '04. 2004, Apr 2004, New Orleans, United States. pp.504-510 Vol.1, 10.1109/ROBOT.2004.1307199 . hal-03844427

**HAL Id: hal-03844427**

**<https://amu.hal.science/hal-03844427>**

Submitted on 14 Nov 2022

**HAL** is a multi-disciplinary open access archive for the deposit and dissemination of scientific research documents, whether they are published or not. The documents may come from teaching and research institutions in France or abroad, or from public or private research centers.

L'archive ouverte pluridisciplinaire **HAL**, est destinée au dépôt et à la diffusion de documents scientifiques de niveau recherche, publiés ou non, émanant des établissements d'enseignement et de recherche français ou étrangers, des laboratoires publics ou privés.

# A miniature biomimetic gaze control system

Stéphane Viollet and Nicolas Franceschini

*Biorobotics Research Group, Movement and Perception Lab.  
CNRS/Univ. de la Méditerranée, 31, chemin Joseph Aiguier  
13402 Marseille, France  
{viollet, franceschini}@laps.univ-mrs.fr*

For any sighted mobile creature, whether it be natural or artificial, stabilizing the visual system is a much more crucial issue than that of preventing a snapshot from being blurred by the unsteadiness of a human photographer. The more immune the eye of an animal or a robot is to various kind of disturbances such as body or head movements of all kinds, the less troublesome it will be for the visual system to carry out its many information processing tasks when walking or flying in unknown environments. The gaze control system that we describe in this paper takes a lesson from the Vestibulo Ocular Reflex (VOR) that is known to contribute to the stabilization of the human eyes. The originality and performances of the control system arise from the merging of two sensory modalities:

- a retinal position signal is yielded by a novel piezo-based visual sensor called OSCAR (Optical Sensor for the Control of Autonomous Robots)
- a VOR reflex is merged with a visual smooth pursuit reflex.

Our gaze controller involves a feedforward eye control based on measurements of the angular head speed by a rate gyro. The performances of the gaze controller were tested on-board a miniature (5 grams) oculomotor system, which makes use of the OSCAR visual sensor. The combined visual/inertial sensory-motor controller enables the gaze to be stabilized within a 12-times smaller range than the perturbing head movements, which were applied here at frequencies of up to 3 Hz with an amplitude of 6° peak-to-peak. This is a relatively high standard of performance in terms of rejecting head movement disturbances; in any case, these performances are comparable to those which the human visual system is capable of.

*Vision, Scanning sensor, Sensorimotor control, Sensory fusion, VOR, Rate gyro, Biorobotics.*

## I. INTRODUCTION

The ability of flying insects to stabilize their visual system in space is a striking example of Nature's know-how in terms of an efficient visually guided system adapted to an autonomous vehicle. As suggested by the fly [1] and dragonfly [2], gaze stabilization was the crucial first step towards achieving the stabilization of a complete Micro Air Vehicle (MAV) around its six degrees of freedom and making it able to track a target during aerobic manoeuvres. The first advantage of uncoupling an eye from its support (be it a head or a body) is that this makes

it possible to maintain the orientation of the gaze even when disturbances affect the eye support. The fly has no less than 23 pairs of micro-actuators (muscles) dedicated to controlling the orientation of its head (and hence that of its eyes) relative to its body [3]. This insect is thus able to compensate for body disturbances in pitch, roll [4] and yaw [5].

If we attempt to take a lesson from Nature, it becomes a real engineering challenge to reach a similar degree of efficiency on-board artificial vehicles. The high level of efficiency of natural gaze control systems is known to rely on their ability to measure disturbances after very short latencies. Studies on the human Vestibulo-Ocular Reflex (VOR) have shown that this inertial system responds efficiently with a latency of only about 10ms to sinusoidal head rotations up to a frequency of 4Hz [6] and to step rotations [7]. The fly itself shows an outstanding VOR-like reflex controlling the orientation of its head. The fly counteracts any body roll movements (up to an amplitude of 180°, 1Hz) by merging its body angular speed measurements (via the halteres) with visual information [4]. Similar compensations occur for yaw motion disturbances, where the head is observed to turn in antiphase with the thorax at speeds of up to 3300°/s [5]. In the field of robotics, few studies have explored the mechanisms involved in this kind of feedforward control undergoing rotational disturbances at frequencies higher than 1Hz. A gaze control system merging a retinal position signal with an inertial measurement was proposed [8]. The performances of the gaze stabilisation were assessed using slow disturbances generated by hand. Shibata and Schaal [9] have described a gaze control system based on an inverse model of the oculomotor plant. This control system, which is enhanced by a learning network, was able to decrease the retinal slip 4-fold in response to a sinusoidal disturbance at 0.8Hz. Likewise, the performances of an adaptive image stabilizer for a robotic agent have been tested with disturbances up to 0.8Hz [10]. The authors of two other studies [11,12] have presented gaze stabilization systems inspired by the human VOR reflex, but the performances of these sensorimotor control systems have not been assessed on a real experimental platform.

In the present study, we equipped an elementary oculomotor plant with rapid gaze stabilization capacities by merging a visual position feedback loop with a feedforward control system inspired by the VOR. In contrast with other studies based on a learning scheme, the VOR-like reflex was achieved by implementing a feedforward control in the simplest possible

way, using frequency compensation as described in a recent dynamic model for the VOR in primates [13]. We designed, constructed and tested a miniature oculomotor system with a single rotational axis (yaw). The front end of this system is a retinal position sensor called OSCAR (Optical Sensor for the Control of Autonomous Robots) [14]. This sensor draws on the results of electrophysiological, micro-optical, neuroanatomical and behavioral studies which were carried out in parallel at our laboratory on the fly visual system [15].

In a first part, we describe the principle and the implementation of the OSCAR sensor, which was redesigned here completely to give a much lighter sensor (4.5 grams). In the second part, we describe the gaze control system. Lastly, we describe the experimental setup we have developed to test the performances of this miniature oculomotor system in the presence of disturbances of various kinds.

## II. OSCAR: A BIO-INSPIRED SCANNING SENSOR

This section describes a new version of the OSCAR sensor, which differs considerably from that presented in previous studies [14,16,17]. We completely redesigned the sensor with an emphasis on the use of a new actuator and a new Elementary Motion Detector (EMD) circuit.

### A. Description of the piezo-based OSCAR sensor

The new OSCAR sensor is based on a miniature microscanning device, the components of which are shown in Fig. 1.

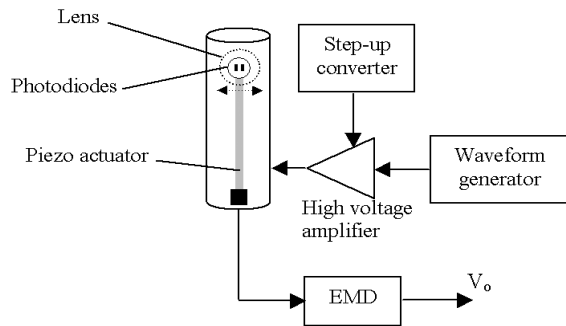


**Figure 1.** Sketch of the piezo-based OSCAR sensor. The actuator that we used to generate the periodic ( $F_{sc} = 10\text{Hz}$ ) scanning movement (indicated by the double arrow) is a multilayer piezoelectric bender giving a deflexion of 1mm for an operating voltage of 60V. It is mounted into an eye tube (diameter 10mm)

This sensor is composed of a miniature lens (diameter 5mm, focal length 8.5mm) and an elementary “retina” composed of only two photodiodes mounted behind the lens after being glued onto the side of a rectangular multilayer bender actuator. The latter is mounted in the center of a thin carbon fiber tube (diameter 10mm). The total mass of this artificial eye is only 4.5 grams. On the basis of previous electrophysiological and

behavioural studies carried out at our laboratory [15], a periodic ( $F_{sc}=10\text{Hz}$ ) scanning movement is imposed on the actuator by a waveform generator circuit. The scan period consists of 2 phases: a first phase (duration 50ms) at a *variable speed* and a return phase (duration 50ms) at a *constant speed* [14,16]. The piezo actuator is controlled here in open loop because the scanning frequency  $F_{sc}$  (10Hz) is much lower than the bandwidth (about 150Hz) of the moving equipment. The voltage of 60V required to obtain the maximum deflection (1mm) of the piezo actuator is obtained by means of a micro step-up converter circuit powering the small high-voltage amplifier that drives the piezo bender. The two photoreceptors therefore scan their optical environment at a frequency of 10Hz with an amplitude of  $10^\circ$ . When placed in front of a contrasting pattern, such as a bar or an edge (see, e.g., Fig. 4), this scanning eye generates an essentially 1D *rotational optic flow* characterized by its angular speed  $\Omega$ . This angular speed is estimated by an Elementary Motion Detector (EMD) driven by the pair of photoreceptors. The EMD circuit outputs a pulse, the duty cycle of which increases with the angular speed  $\Omega$ . We recently designed a new version of the EMD based on the same working principle as the previous one (the principle that we originally developed in the 1980's based on our analysis of the fly's EMDs with single photoreceptor stimulation), but which uses a tiny microprocessor, giving a major reduction in size (5.4cm<sup>2</sup>) and mass (0.8g) [18]. The whole OSCAR sensor, with its optics, piezo actuator, wiggling retina, EMD circuit and drive electronics weighs only 8grams. It features a much larger bandwidth than its forerunner and could therefore be used to scan the surroundings at frequencies greater than 10Hz. This larger bandwidth was also the key to the simplified electronics, as it did away with the need for a position feedback loop.

### B. OSCAR: an angular position sensor

We calibrated the new OSCAR sensor by rotating it stepwise around the vertical axis in front of a fixed target (a vertical edge) posted on a wall, 130cm ahead, while monitoring the response at each azimuthal orientation. Figure 2 shows an example of the static *characteristic curves* obtained. The responses happen to be quasi-linear functions of the azimuthal orientation  $\theta_i$  of the sensor with respect to the target (an edge). They were fairly insensitive to the contrast down to  $m = 0.4$ . Like its forerunner, this new OSCAR sensor boasts an exquisite angular accuracy at the task of *locating* an edge or a bar: approximately  $0.1^\circ$ , an angle which is 40 times smaller than the interreceptor angle  $\Delta\phi$  ( $\Delta\phi = 4^\circ$  here). OSCAR can therefore be said to be endowed with *hyperacuity*.

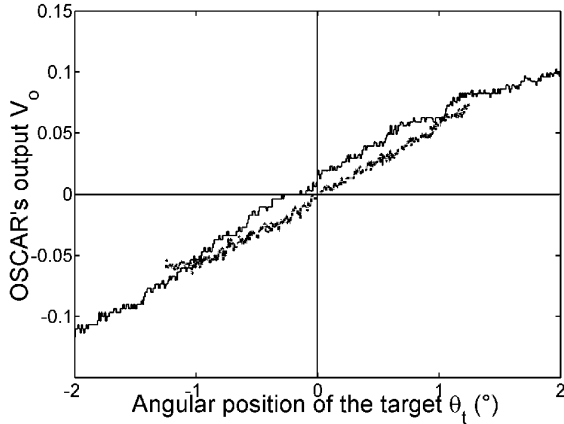


**Figure 2.** The OSCAR sensor's output  $V_o$  as a function of its azimuthal orientation  $\theta_t$ , with respect to the target: a grey vertical edge posted on a white background at a distance of 130cm (thin line: edge contrast  $m = 85\%$ ; bold line: edge contrast  $m = 40\%$ ).

### B. Implementation of an OSCAR-based oculomotor plant

Figure 3 shows a sketch (top view) of the oculomotor system that we designed and built at our laboratory.

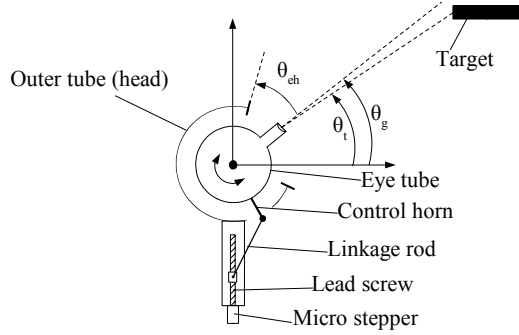


**Figure 3.** The eye tube (represented at scale 1:1) is inserted into a larger carbon tube (called "the head") within which it can turn freely on pivot bearing around its vertical axis. This configuration allows one degree of freedom (DOF) between the OSCAR eye and the head. One step of the micro stepper leads (via the lead screw, the linkage rod and the control horn) to a rotation of the eye in head by  $\approx 0.15^\circ$ .

The outer carbon tube (Fig. 3,4) with its circular electronic boards can be said to correspond to the "head", within which the OSCAR eye tube can turn freely.

To move the eye in the head, we needed an actuator giving a high angular resolution, of the order of  $0.2^\circ$ . We constructed a micro actuator based on a lead screw (diameter 2mm, pitch 0.4mm) mounted onto the shaft of a micro step motor (Sanyo), as sketched in Fig.3 and in the inset of Fig. 5. A brass nut driven by the screw drives the eye via a 0.4mm linkage rod and a control horn glued to the inside tube (the eye). The eye is driven within the head (angle noted  $\theta_{ch}$ ) with an angular resolution of

$0.15^\circ$  per motor step.

### III. OPTOMOTOR RESPONSE IN YAW

The vision system described in section II was mounted onto the shaft of a low friction resolver (Fig. 4). The complete electronics were made with Surface Mounted Devices (SMD). The SMD electronic components occupy two printed circuit boards (diameter of 45mm) which are supplied directly by batteries. Each board is dedicated to a particular task, as follows:

Board 1: electronic circuits driving the piezo actuator

Board 2: conditioning circuits and EMD circuit.

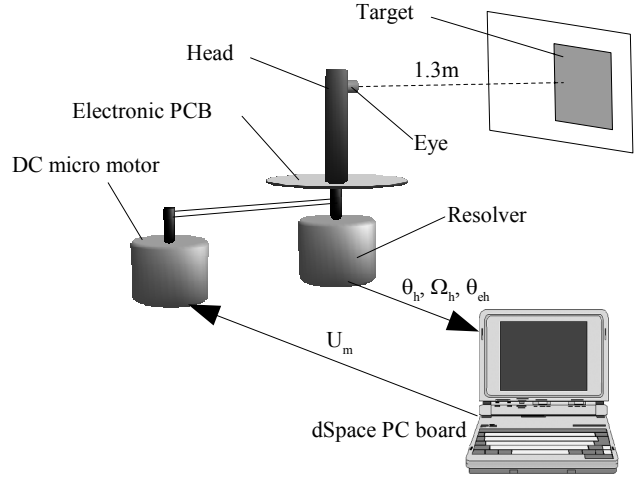


**Figure 4.** Sketch of the testbed that was used to assess the performances of the gaze control system. The angular position  $\theta_h$  and the angular speed  $\Omega_h$  of the support were measured using a low friction, low inertia resolver. To test the performances of the gaze control system, the head with the electronics is mounted onto the shaft of a low friction resolver coupled via a belt to a zero backlash DC micromotor. The latter applies rotational disturbances (step or sinusoidal disturbances) to the head via the control input  $U_m$ .

The use of a very tiny Cygnal micro-controller (3 by 3mm) enabled us to greatly reduce the area occupied by the electronics. In the first step, the controller of each feedback loop (the visual and inertial loops) was implemented and tested on a dSpace dedicated PC board. Although this board is completely integrated into the Matlab/Simulink environment, all the most crucial tasks are performed in real time on a microprocessor included with the board. This configuration enabled us to adjust the parameters of the controllers on the fly regardless of the timing imposed by the PC operating system.

For testing the performances of the overall system, the orientation of the oculomotor plant is controlled by a DC micro motor coupled via a frictionless belt and monitored by the resolver. The micromotor + reduction gear selected (Minimotor) has zero backlash and therefore does not introduce any nonlinearity such as hysteresis (the adverse effects of which would occur when the direction of rotation is switched). A reference input to this servo-loop enables the head to be driven

sinusoidally at various frequencies in the range 0-5Hz. Alternatively aperiodic steps with rise time as small as 70ms are applied, which suddenly disturb the gaze orientation.

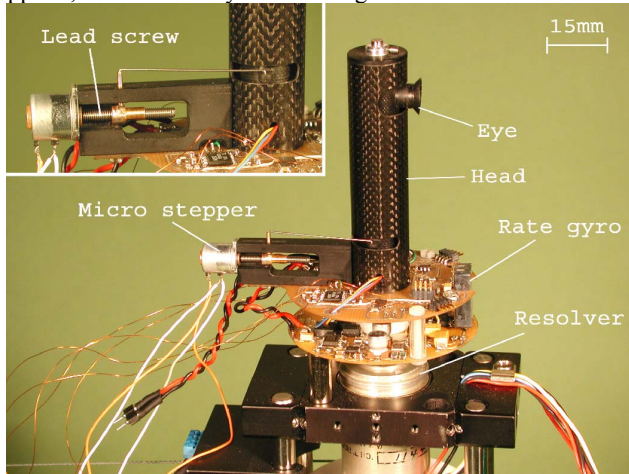


**Figure 5.** The complete oculomotor system composed of the OSCAR visual sensor (the "eye") which can rotate within an outer tube (the "head") as sketched in Figure 3.

#### A. Dynamics of the gaze controller

The control of the azimuthal orientation of the eye in space (i.e., the gaze noted  $\theta_g$ ) results from the fusion between a visual *feedback loop* and a *feedforward control* of the angular position of the eye  $\theta_{eh}$ . The latter control system is based on the measurement of the angular velocity of the head  $\Omega_h$  (VOR-like control). Special attention was paid to modelling the inertial sensor and the eye's dynamics so as to be able to tune accurately the various parameters of the feedforward controller.

##### 1. Model of the oculomotor plant and its inertial sensor

The dynamics the oculomotor plant was modelled from its response to a chirp input signal (amplitude  $5^\circ$ , starting frequency 0.1Hz, ending frequency 5Hz, reached in 60s). The maximum rotational speed that the step motor can yield is equal to 1200 steps/s which is equivalent to an angular head speed of  $180^\circ/s$  (one step is equal to a rotation of the eye of  $0.15^\circ$ ). Up to this maximal speed, the step motor and thus the oculomotor plant model can be considered as a simple gain noted  $K_e$ . If higher speeds than  $120^\circ/s$  are required to turn the eye, the step motor will run in a saturated mode. This is a limitation of this oculomotor plant which can not generate rotations as fast as those of the human ocular saccades (which reach an angular speed of  $350^\circ/s$  [19]).

As shown in figure 5, we have mounted a rate gyroscope onto the PCB integrated with the head. This inertial sensor has the same functionality as in the mammalian VOR: it measures the angular speed of the head. This information is used to generate adequate compensation signal at the oculomotor plant level. As

the VOR relies on a feedforward path, it is crucial to model the transfer function  $H(s)$  of the rate gyro accurately. Again, we used the same chirp as previously to obtain a model of the inertial sensor, given by

$$H(s) = K_g \frac{(s - s_1)}{((s + s_2)(s + s_3))} \quad (1)$$

with  $K_g = 731.10^3$ ,  $s_1 = 0.3527$ ,  $s_2 = 458$  and  $s_3 = 528$

From (1),  $H(s)$  is a pseudo-derivator cascaded with two low-pass filters (cut-off frequencies of 73Hz and 84Hz).

#### 2. The overall gaze control system

The various parts of the control scheme that we designed and implemented are depicted in Fig. 6.

Fig. 6 makes explicit that the control signal  $U_e$  that ultimately drives the orientation of the eye results from a simple subtraction between two *position* signals:

- $U_{VOR}$ , a position signal derived from the VOR inertial sensor
- $U_v$ , a position signal derived from the OSCAR visual sensor.

To prevent runaway of the eye when it loses sight of a target, we developed [17] a special limiter, called a Zero-Setting Limiter (ZSL), shown in Fig. 6. The ZSL clamps the error signal back to zero whenever the latter tends to become higher (or lower) than a specified positive (or negative) level.

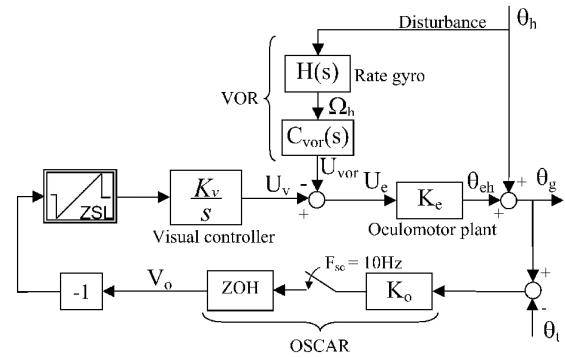


**Figure 6.** Block diagram of the gaze control system which maintains the gaze on the (stationary or moving) target despite head disturbances. This system is composed of a visual feedback loop based on the OSCAR visual sensor ("optical position sensor") and a feedforward mechanism emulating a VOR reflex. The controller  $C_{vor}$  integrates the angular speed signal  $\Omega_h$  delivered by a rate gyro. The VOR reflex is combined with the smooth pursuit reflex by simply subtracting the control signal  $U_{vor}$  from  $U_v$  together to drive the eye in the head ( $\theta_{eh}$ ).

From Fig. 6 and for  $U_v = 0$ , we have

$$\theta_{eh} = -H(s)C_{vor}(s)K_e\theta_h. \quad (2)$$

To obtain a perfect VOR compensation for a head rotational disturbance, the angular orientation of the eye  $\theta_{eh}$  must vary in opposition with  $\theta_h$ . From (2),  $\theta_{eh} = -\theta_h$  if

$$C_{vor}(s) = \frac{1}{(H(s)K_e)} \quad (3)$$

We used a lag compensator instead of a pure integrator to obtain a stable control input  $U_{vor}$ . We therefore approximated from its frequency response the feedforward controller  $C_{vor}(s)$  given in (2) by the controller noted  $\tilde{C}_{vor}(s)$  as follows

$$\tilde{C}_{vor}(s) = K_{vor} \frac{(s+a)}{(bs+1)} \quad (3)$$

The transfer function of each controller was digitized (at a sampling frequency of 1kHz) using Tustin's approximation method and implemented directly in its discrete form.

To summarize, the input  $U_c$  constitutes a positional error signal that sets the micro stepper into motion to compensate for the movement of either the target (visual disturbance  $\theta_t$  in Fig. 6) or the head (inertial disturbance  $\theta_h$  in Fig. 6). A displacement of the target ( $\theta_t$ ) will trigger smooth pursuit, whereas an untimely rotation of the head ( $\theta_h$ ) will lead to VOR compensation.

### B. Rejecting rotational disturbances by merging VOR and smooth pursuit reflexes

The performances of the gaze controller in rejecting head disturbances and maintaining a fixed gaze were analysed by applying two kinds of disturbance to the head: a step displacement of  $3^\circ$  and a sinusoidal displacement of  $6^\circ$  peak-to-peak. The feedforward controller  $C_{vor}(s)$  was adjusted so as to minimize the retinal slip error in the 0.1Hz - 3Hz frequency range.

Fig. 6 clearly shows that turning the head by an angle  $\theta_h$  creates a disturbance for both controllers  $C_{visual}$  and  $C_{vor}$ . Accordingly, the response of this system (in terms of the angular rotation of the eye in the head:  $\theta_{eh}$ ) to an angular step displacement  $\theta_h$  of the head can be decomposed into two parts (see the curve  $\theta_{eh}$  in Fig. 7):

- a *transient* part corresponding to the *inertial* pathway (VOR), which benefits from the fast dynamics associated with this pathway (where the lag time is only about 10ms)
- a *steady* part corresponding to the *visual* pathway, which suffers from the relatively long lag time (100ms) with which the OSCAR visual sensor operates.

As a result, the gaze stays seemingly frozen in space, as shown by the curve  $\theta_g$  (Fig. 7), which was obtained simply by summing together the two curves  $\theta_h$  and  $\theta_{eh}$ . The advantage of this system is that the gaze hardly departs from the target, in spite of the fact that the head rotation vastly overshoots the extent of the visual field ( $\pm 2.5^\circ$ ) of the visual sensor. Hence, the remarkable, human-like compensatory effect illustrated in Fig. 7 is due to the fact that the fast, albeit rather inaccurate response of the VOR most conveniently complements the low bandwidth but accurate response of the visual feedback loop.

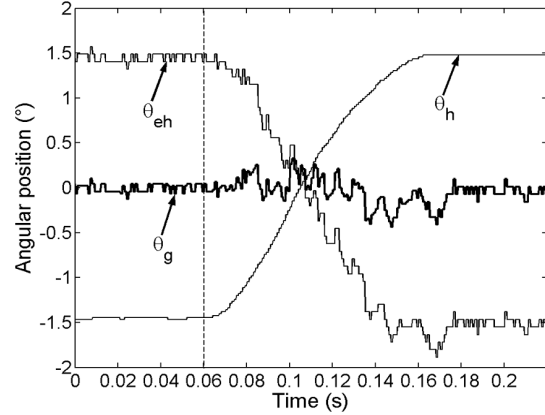


**Figure 7.** Response of the miniature gaze control system shown in Fig. 5 to an abrupt  $3^\circ$  step rotation of the head ( $\theta_h$ ). The response is measured by monitoring the angular position of the eye with respect to the head ( $\theta_{eh}$ ) by means of a tiny magnetic sensor mounted onto the head PCB. The gaze response ( $\theta_g$ ), obtained by summing the two curves, shows that the maximum deviation of the gaze ("eye in space") is at most  $0.4^\circ$ . The vertical dashed line indicates the instant at which the step was applied.  $A = 60$ ,  $b = 5$ ,  $K_v = 333$ ,  $K_o = 0.05$ ,  $K_e = 0.15$  and  $K_{vor} = 0.77$ .

In the second step, we applied a sinusoidal head disturbance  $\theta_h$  to the oculomotor plant. As a result (Figure 8), even a relatively fast sinusoidal disturbance (2Hz) imposed upon the head is immediately compensated for by an antiphase counter-rotation of the eye, which eventually makes the gaze (the eye in space  $\theta_g$ ) deviate only very slightly: the *rms* value of  $\theta_g$  is only  $0.23^\circ$ , which is 25 times smaller than the applied head disturbance ( $6^\circ$  peak-to-peak).

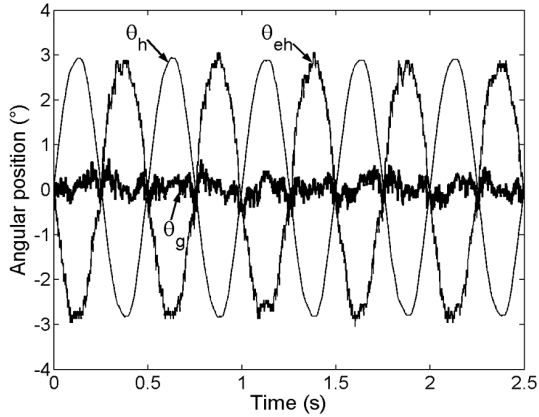


**Figure 8.** Response of the miniature gaze control system shown in Fig. 5 to a sinusoidal head disturbance with a relatively large amplitude ( $\theta_h = 6^\circ$  peak-to-peak) applied at a relatively high frequency (2 Hz). The gaze signal  $\theta_g$ , corresponding to the direction of the visual axis in space ("eye in space"), was obtained by summing together the two curves ( $\theta_h + \theta_{eh}$ ). This gaze angle  $\theta_g$  hardly departs from zero in spite of the severe head disturbance applied. The retinal slip ( $0.23^\circ$  rms, as determined during a 20 second recording period) is here 25 smaller than the applied head disturbance. The visual system keeps fixating the dark contrasting edge 1.3 meters ahead.  $a = 60$ ,  $b = 5$ ,  $K_v = 0.05$ ,  $K_c = 333$ ,  $K_e = 0.15$  and  $K_{vor} = 0.77$ .

Fig. 9 shows the rms value of the gaze  $\theta_g$  at various periodic head rotation frequencies.

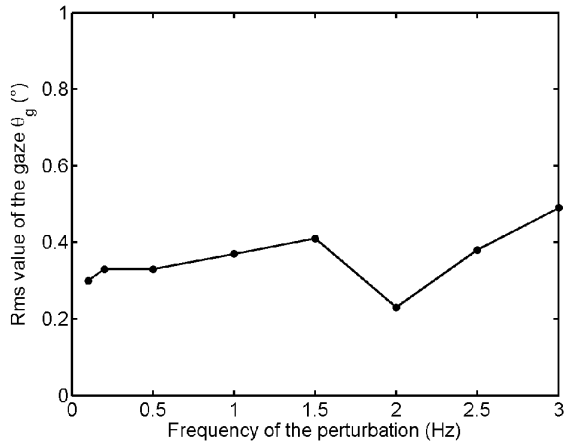


**Figure 9.** Root-Mean-Square (rms) value of the gaze angle  $\theta_g$  (eye in space) with respect to sinusoidal disturbances applied to the head at various frequencies.  $\theta_g$  was obtained by summing together the two curves  $\theta_h + \theta_{eh}$ , as in Figure 8. The rms value of  $\theta_g$  was calculated during a 20-second recording period and normalized with respect to a  $6^\circ$  peak-to-peak disturbance amplitude.

The root-mean-square excursion of the gaze signal  $\theta_g$  was never higher than  $0.5^\circ$  up to a frequency of about 3Hz (Fig. 9). This shows how efficiently the system rejects head rotational disturbances, especially considering that at 3Hz, the head

reaches angular speeds of the order of  $60^\circ/s$ . By comparison, the maximum frequency of the disturbances that the visual feedback loop alone can reject (without VOR) is only about 0.5Hz, and even then, at the expense of a large retinal slip error. Figures 8 and 9 therefore illustrate the strikingly effective way in which the system compensates for the untoward effects of head movements on the gaze.

#### IV. CONCLUSION

Here we described the implementation of a fast oculomotor system that draws its inspiration from highly proficient, long existing biological systems that have stood the test of time. We first described a novel version of our OSCAR visual sensor, the basic principle of which now comes even closer to that underlying the housefly's retinal scanner [14], since the scan now involves the retina proper and not the whole eye. This new version is a major improvement over the previous one [13,15]. In particular, the use of a cantilever piezoactuator for imposing a specific scanning movement on the retina behind the lens is a highly valuable solution because :

- the mass of the scanning eye was reduced about 3-fold (4.5g versus 14g in the OSCAR original version),
- the power consumption was reduced about 20-fold (0.14W versus 2.4W in the former version),
- the scanning frequency is still 10Hz but it can now be easily increased to 40Hz, which would reduce the visual sensor's lag time to about 25ms.
- the control scheme was simplified because the larger bandwidth of the piezo-scanner made the position feedback loop present in the former OSCAR version unnecessary,
- the linearity of the OSCAR characteristic sensor curve was greatly improved

These many improvements have not affected the high accuracy with which the OSCAR sensor is able to *locate* a contrasting edge: the accuracy is still about  $0.1^\circ$  in the new OSCAR version and this is still 40 times better than what might be expected in view of the low static resolution of the eye ( $\Delta\varphi = 4^\circ$ ). This high accuracy in the angular *localisation* of an object is a property called *hyperacuity*. The new piezo-based version of the OSCAR sensor can therefore be said to be a really valuable angular position sensing device that can deal with natural contrasting features in the nearby environment.

Secondly, we have described an efficient gaze control system based on the fusion between a visual feedback loop and a feedforward control system inspired by the human Vestibulo Ocular Reflex (VOR) and the fly haltere system. The structure of the gaze control system was relatively easy, owing to the excellent performances of the actuator (i.e., the stepper motor) used to control the orientation of the eye in space (i.e., the gaze). The dynamic model of the oculomotor system includes only a simple gain in the bandwidth of interest in this study (0-5Hz). The overall gaze control system does not require large

computational resources. It can be implemented easily, for example on a small, low-cost, low-weight 8-bit micro-controller.

We have given two examples of how this control system generates fast compensatory eye movements which appropriately reject yaw disturbances applied to the support (called “the head”):

- a large step rotation of the head by  $3^\circ$  (a value which actually exceeds the angular range of the OSCAR sensor) is rejected so as to leave the eye with a retinal slip no larger than  $0.4^\circ$  at any time (Fig. 8)
- a large sinusoidal rotation of the head by  $6^\circ$  peak-to-peak (which goes far beyond the angular range of the OSCAR sensor) is rejected in the 0.1Hz to 3Hz range, leaving the gaze stabilized within a range as small as  $0.5^\circ$ , which is 12 times smaller than the amplitude of the disturbance (Figures 8, 9).

The design of the miniature gaze control system presented here is simpler than that of the eye/head system of vertebrates, where the axis of rotation of the eyeball is not confused with that of the head. We have focused our efforts on the design and the construction of the eye so as to minimize the mechanical nonlinearities introduced by the actuator and the optical nonlinearity introduced by the off-axis effects. Our system therefore does not require any continuous feedforward gain adjustments to compensate for the off-axis effects which gave rise to the most significant nonlinearities in the classical eye/head configuration [9,10].

The development of a micro gaze control system turns out to be crucial for the visual stabilization of future robotic platforms. All-terrain wheeled robots and legged robots for terrestrial and extra-terrestrial operations inherently suffer from gaze disturbances induced by their locomotor apparatus and by the “unprepared” nature of the terrain they have to cover. Likewise, unmanned air vehicles (UAVs) and micro-air vehicles (MAVs) have to cope with the dramatic disturbances caused, for instance, by the fast airfoil pitch variations, wing-beats, and all kinds of unpredictable aerodynamic disturbances. Nature teaches us that these disturbances ought to be blocked at an early stage, simply to reduce the processing load imposed on the visual system.

Although we have dealt here with disturbance rejections around the yaw axis, disturbances can affect all the rotational degrees of freedom of an eye. Further research is now required before perfect eye stabilisation can be achieved around the various rotational degrees of freedom.

#### ACKNOWLEDGEMENT

The authors would like to acknowledge the assistance of M. Boyron and S. Amic, who constructed the two miniature electronic boards including the piezo driver and the EMD. We wish to thank F. Paganucci for his help in the construction of the eye and C. Vuilmet, who designed the stepper drive electronics. We also thank F. Ruffier for fruitful discussions and comments and J. Blanc for improving the English manuscript. This work was supported by CNRS (Life Sciences, Engineering Sciences,

Microsystem and Microbotic Programs) and by a European Union contract (IST/FET- 1999-29043).

#### REFERENCES

1. J. H. Van Hateren and C. Schilstra, “Blowfly flight and optic flow. II. Head movements during flight”, *J of Exp Biol*, vol. 202, pp. 1491-1500, 1999.
2. R. M. Olberg, A. H. Worthington, and K. R. Venator, “Prey pursuit and interception in dragonflies,” *J Comp Physiol A*, vol. 186, pp. 155-162, 2000.
3. N. J. Strausfeld, H. S. Seyan, and J. J. Milde, “The neck motor system of the fly *Calliphora erythrocephala*,” *J Comp Physiol A*, vol. 160, pp. 205-224, 1987.
4. R. Hengstenberg, “Mechanosensory control of compensatory head roll during flight in the blowfly *Calliphora erythrocephala* Meig.,” *J Comp Physiol A*, vol. 163, pp. 151-165, 1988.
5. D. C. Sandeman, “Angular acceleration, compensatory eye movements and the halteres of flies (*Lucilia serricata*),” *J. Comp. Physiol. A*, vol. 136, pp.361-367, 1980.
6. S. Tabak, and H. Collewijn, “Human vestibulo-ocular responses to rapid, helmet-driven head movements,” *Exp Brain Res*, vol. 102, pp.367-378, 1994.
7. E. F. Maas, W. P. Huebner, S. H. Seidman and R. J. Leigh, “Behavior of human horizontal vestibulo-ocular reflex in response to high-acceleration stimuli,” *Brain Research*, vol. 499, pp.153-156, 1989.
8. T. Yamaguchi, and H. Yamasaki, “Active vision system integrated with angular velocity sensor,” *Measurement*, vol. 15, pp.59-68, 1995.
9. T. Shibata, and S. Schaal, “Biomimetic gaze stabilization based on feedback-error learning with nonparametric regression networks”, *Neural Networks*, vol. 14, pp.201-216, 2001.
10. F. Panerai, G. Metta, and G. Sandini, “Learning visual stabilization reflexes in robots with moving eyes,” *Neurocomputing*, vol. 48(1-4), pp. 323-337, 2002.
11. P. Viola, “Neurally inspired plasticity in oculomotor processes,” in *Neural Informations Processing Systems*, 1989, pp. 290-297.
12. A. Lewis, “Visual navigation in a robot using Zig-Zag behavior,” in *Neural Informations Processing Systems*, 1997, pp. 822-828.
13. Y. Hirata, I. Takeuchi, and S. M. Highstein, “A dynamic model for the vertical vestibuloocular reflex and optokinetic response in primate,” *Neurocomputing*, Vol. 52-54, pp. 531-540, 2003.
14. S. Viollet, and N. Franceschini, “Biologically-inspired visual scanning sensor for stabilization and tracking,” in *Proceedings of IEEE IROS'99*, Kyongju, Korea, 1999, pp. 204-209.
15. N. Franceschini, and R. Chagneux, “Repetitive scanning in the fly compound eye,” in *Göttingen Neurobiology Report*, Thieme, Stuttgart, 1997, vol. 2, pp. 279.
16. S. Viollet, and N. Franceschini, “Visual servo system based on a biologically-inspired scanning sensor,” in *Proc of SPIE Conf on Sensor fusion and decentralized control in robotics II*, Boston, USA, vol 3839, 1999, pp.144-155.
17. S. Viollet, and N. Franceschini, “Super-accurate visual control of an aerial minirobot”, in *Autonomous Minirobots for Research and Education AMIRE*, U. Rückert, J. Sittte and U. Witkowski (Eds), Heinz Nixdorf Institute, Paderborn, Germany, 2001, pp. 215-224.
18. F. Ruffier, S. Viollet, S. Amic, and N. Franceschini, “Bio-inspired optic flow circuits for the visual guidance of micro-air vehicles,” in *IEEE Int Symposium on Circuits and Systems ISCAS'2003*, Bangkok, Thailand, 2003, pp. 846-849.
19. R. J. Leigh, and D. S. Zee, *The neurology of eye movements*, Oxford University Press, 1999.